

This article was downloaded by: [Siauliu University Library]

On: 17 February 2013, At: 07:04

Publisher: Taylor & Francis

Informa Ltd Registered in England and Wales Registered Number: 1072954

Registered office: Mortimer House, 37-41 Mortimer Street, London W1T 3JH, UK



Advanced Composite Materials

Publication details, including instructions for authors and subscription information:

<http://www.tandfonline.com/loi/tacm20>

Bearing failure in bolted composite joints: analytical tools development

Yi Xiao & T. Ishikawa

Version of record first published: 02 Apr 2012.

To cite this article: Yi Xiao & T. Ishikawa (2002): Bearing failure in bolted composite joints: analytical tools development , Advanced Composite Materials, 11:4, 375-391

To link to this article: <http://dx.doi.org/10.1163/156855102321669190>

PLEASE SCROLL DOWN FOR ARTICLE

Full terms and conditions of use: <http://www.tandfonline.com/page/terms-and-conditions>

This article may be used for research, teaching, and private study purposes. Any substantial or systematic reproduction, redistribution, reselling, loan, sub-licensing, systematic supply, or distribution in any form to anyone is expressly forbidden.

The publisher does not give any warranty express or implied or make any representation that the contents will be complete or accurate or up to date. The accuracy of any instructions, formulae, and drug doses should be independently verified with primary sources. The publisher shall not be liable for any loss, actions, claims, proceedings, demand, or costs or damages whatsoever or howsoever caused arising directly or indirectly in connection with or arising out of the use of this material.

Bearing failure in bolted composite joints: analytical tools development

YI XIAO* and T. ISHIKAWA

Advanced Composites Evaluation Technology Center, National Aerospace Laboratory of Japan (NAL), 6-13-1 Osawa, Mitaka-shi, Tokyo 181-0015, Japan

Received 24 May 2002; accepted 18 December 2002

Abstract—This paper presents an analytical tool development for simulating the bearing failure and response of bolted composite joints. It is implemented into a general-purpose finite element code ABAQUS. The main damage mechanisms observed from the experiments are described as accumulated compressive damage, induced by shear and compression failures of fiber and matrix. The contact problem at the pin/hole boundary, progressive damage, finite deformation and nonlinear material behavior are taken into account when developing the analytical tool. A complex approach based on a nonlinear shear elasticity theory combined with a continuum damage mechanics approach can also be utilized to represent the nonlinear material behavior during loading. The damage accumulation criteria based on the hybrid failure criteria of Hashin and Yamada-Sun are adopted, and a degradation model for the damaged ply is proposed for the stress redistribution analysis. The computed results, including progressive damage and strength response of the joints, agreed well with the existing experimental data.

Keywords: CFRP laminated composites; bearing failure; progressive damage; continuum damage mechanics (CDM).

1. INTRODUCTION

Carbon fiber reinforced polymeric composite materials have been applied extensively to both primary and secondary structures of the next generation supersonic transport aircraft. In these structures, joining by mechanically fastened joints is a common technology for assembling structural components, and is also the most challenging problem among engineering mechanics specialists. Hence, if the design for the mechanically fastened joints were inadequate, such joints would not only become frequent sources of failure in composite structures, but also could directly affect the durability and reliability of aircraft structures.

*To whom correspondence should be addressed. E-mail: xiaoyi@nal.go.jp

Recently, a method that combines the concept of continuum damage mechanics (CDM) [1] with finite element method (FEM) has been applied in failure analysis of mechanically fastened composite joints. Several analytical models have also been developed and documented in Refs [2–6]. In the damaged accumulation model, it was found that the description of the material degradation due to damage is critical for the stress redistribution analysis. However, since the simple model was used to discuss the effect of accumulated damage on the material degradation of laminated composites, it was impossible for the presented models described above to reproduce the bearing damage process covering the final structural failure. In practice, based on experimental observation [7], it was shown that the bearing failure and response of bolted composite joints are strongly affected by the lateral constraints, and this tends to prevent the reduction of the in-plane stiffness of laminates. Hung and Chang [5] presented a two-dimensional damage accumulation model, the effects of clamping pressure and lateral constraints on bolted joints have been taken into account in their model. However, since the critical bearing damage area in bolted composite joints was not fully clarified, further modification of the material degradation rule will be necessary.

The objective of this research work is to develop an analytical tool for predicting the response and bearing failure of bolted composite joints. This tool will be designed such that it is easy to implement and use, and requires minimum number of input parameters. In order to accurately simulate the bearing damage behavior, the basic damage mechanisms and mechanics governing the bearing failure based on the experimental observation are considered. The accurate prediction results including the progressive damage and strength response of the joints, and the effectiveness of the stiffness degradation models proposed in this paper will be presented and discussed.

2. STIFFNESS REDUCTION MECHANISMS

In order to evaluate the relationship between the bearing strength and damage progress behavior in the bolted composite joints, a detailed experimental investigation has been performed in the authors' previous works, see Ref. [7] for more details.

Two material systems selected for comparing the bearing strength in our experimental program were the toughened Graphite/PIXA IM-7/PIXA and brittle Graphite/Epoxy IM600/Q133. Both composites were quasi-isotropic $[45/0/-45/90]_{2S}$ laminate with the same lay-ups. The geometrical configuration and testing setup of the joint specimens are depicted in Fig. 1. A double shear-lap bolted joint fixture was designed for the bearing tests. All specimens designed had width-to-diameter ratio (W/d) of 8, edge-distance-to-diameter ratio (e/d) of 3 and length of 110 mm.

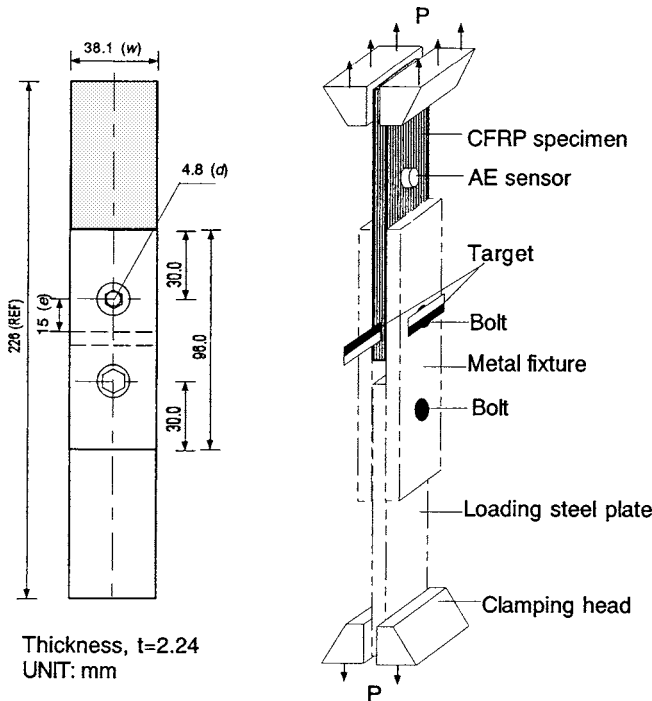


Figure 1. Geometrical configuration and testing setup of bolted joint specimens.

Figure 2 shows the relationship between the strength response and damage. The major characteristics of the bearing damage progression can be summarized as follows.

The bearing failure results in a process of compressive damage accumulation and occurs in four stages: damage onset, damage growth, local fracture and structural fracture (see Fig. 2). Fiber micro-buckling and matrix cracking appear to be the dominant mode in the onset of damage. Out-of-plane shear cracks and delamination are the major modes in the final failure stage. The lateral constraint and the ‘toughness’ of different matrix-based laminates should also influence the bearing failure and damage mechanism. In addition, it was shown that the development of the accumulated damages resulted from fiber micro-buckling, fiber–matrix shearing and matrix compression failure in each individual ply of the laminates. Therefore, the focus of this study is to develop a two-dimensional model capable of predicting the bearing failure and stiffness response for the mechanically fastened composite joints. Bearing failure in laminated composites can be classified in two basic in-plane failure modes: matrix compression and fiber compression-shear failure. Through-thickness shear cracks and delamination, which is an out-of-plane failure mode that may appear in the laminates, is outside the scope of this work, and so will not be considered in this paper.

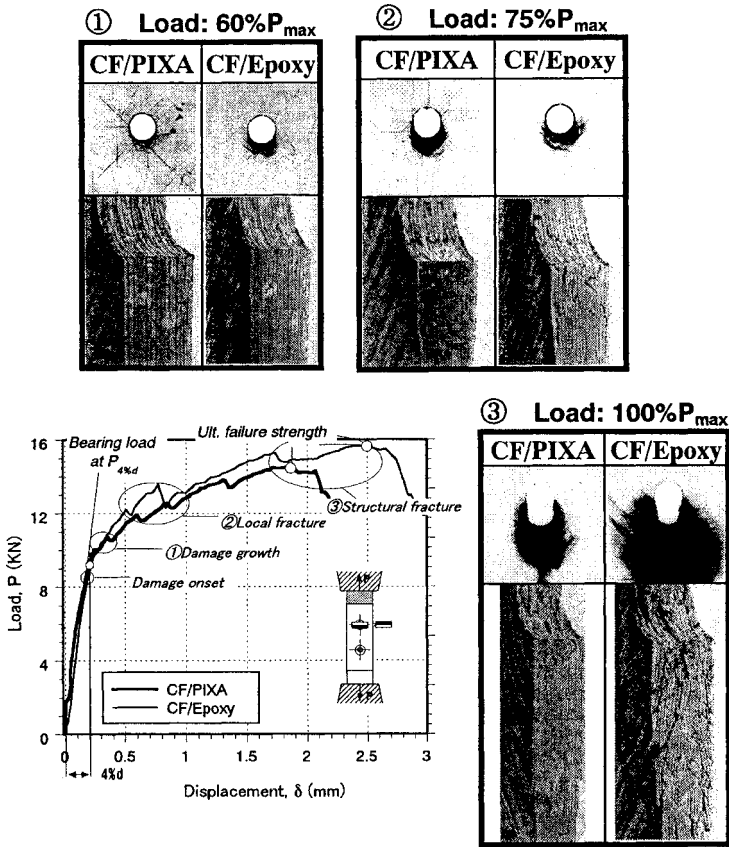


Figure 2. Characteristics of strength response and damage progression observed in the bearing tests for CF/PIXA and CF/Epoxy specimens.

3. ANALYTICAL MODELING

In order to appropriately simulate the nonlinear response of laminated composites, the analytical modeling should take into account two kinds of nonlinearity. One is a nonlinear shearing deformation behavior of the unidirectional composite, which is unrelated to the damage, and the other one is the degradation of material properties caused by the damage.


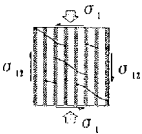
3.1. Nonlinear shear constitutive relationship

It is well known that a composite lamina shows nonlinear behavior in the shear deformation along the fiber direction without damage [8]. Hahn and Tsai formulated the nonlinear shear stress/strain relationship using a high-order elasticity theory [9], which can be written in a simple form,

$$\varepsilon_{12} = G_{12}^{-1} \sigma_{12} + \alpha \sigma_{12}^3, \quad (1)$$

Table 1.

Relationship between failure criteria and damage variable used in progressive damage simulation

Failure mode	Failure index	Damage variable
 <p>Matrix compression failure</p>	$\sigma_2 \leq 0,$ $e_m^2 = \left(\frac{\sigma_2}{Y_c}\right)^2 + \left(\frac{\sigma_{12}}{S_c}\right)^2$ Hashin failure criteria	FV_1 (D_2, D_6)
 <p>Fiber compression-shear failure</p>	$\sigma_1 \leq 0,$ $e_{fs}^2 = \left(\frac{\sigma_1}{X_c}\right)^2 + \left(\frac{\sigma_{12}}{S_c}\right)^2$ Yamada-Sun failure criteria	FV_2 (D_1, D_2, D_6)

where G_{12} , σ_{12} , ε_{12} are the initial ply shear modulus, shear stress and shear strain, respectively, and α represents a nonlinear parameter constant of the material that has to be determined experimentally. The function of equation (1) has to be rewritten in the following incremental form, which will be implemented in a finite element program,

$$\sigma_{12}^{(i+1)} = \frac{1 + 2\alpha(\sigma_{12}^{(i)})^3(\varepsilon_{12}^{(i+1)})^{-1}}{1 + 3\alpha G_{12}(\sigma_{12}^{(i)})^2} G_{12} \varepsilon_{12}^{(i+1)}. \quad (2)$$

3.2. Damage mechanics evolution

Damage progression analysis presented in this paper is similar to the damage-mechanical expression technique reported in references [10, 11]. The procedure is as follows: a stress analysis by the finite element method is initially performed, followed by application of a set of failure criteria to detect the damage of each element, and finally reduction of the material property of the damaged elements. This procedure is repeated for increasing load levels until the properties have been degraded such that the joint fails.

Based on the experimental observation that was described in the previous sections, bearing failure is primarily dominated by the matrix and fiber compression damage. Therefore, an accumulative damage model will be developed to predict the matrix compression and fiber compression-shear failure of a ply in a laminate. For each failure mode, the relationship between failure criteria and damage variable is shown in Table 1, where FV_i are the internal field variables representing the damaged state of lamina. Here FV_1 and FV_2 are defined as the matrix compression and fiber compression-shear failure, respectively, and D_i is the material degradation factor as described in equation (5). The hybrid method based on Hashin and Yamada-Sun's

failure criteria [12, 13] is adopted for predicting damage accumulation in each ply of laminate, containing matrix compression and fiber compression-shear failure. As the failure index (e_m, e_{fs}) exceeds 1.0, the material properties are reduced according to the degradation factors D_i .

3.3. Accumulated damage and property degradation rule

Once the failure takes place in laminated composites, the material properties will be degraded in the damaged area. Based on the modified classical lamination theory, including a nonlinear shear deformation, the stress-strain relations of each lamina in symmetric laminate can be presented as

$$\begin{Bmatrix} \sigma_1 \\ \sigma_2 \\ \sigma_{12} \end{Bmatrix} = \begin{bmatrix} Q_{11}^0 & Q_{12}^0 & 0 \\ Q_{12}^0 & Q_{22}^0 & 0 \\ 0 & 0 & Q_{66}^0 \end{bmatrix} \begin{Bmatrix} \varepsilon_1 \\ \varepsilon_2 \\ \varepsilon_{12} \end{Bmatrix} + f(\varepsilon_{12}) \begin{Bmatrix} 0 \\ 0 \\ \varepsilon_{12} \end{Bmatrix}, \quad (3)$$

where $f(\varepsilon_{12})$ is the real root of the equation (based on Ref. [9]),

$$y^3 + \frac{3}{S_{66}} y^2 + \left(\frac{3}{S_{66}^2} + \frac{S_{66}}{S_{6666}} \frac{1}{\varepsilon_{12}^2} \right) y + \frac{1}{S_{66}^3} = 0. \quad (4)$$

Consequently, the third line of equation (3) shows the inverse of equation (1).

Note that Q_{ij}^0 of equation (3) is the stiffness component that remained unchanged as the original undamaged properties were retained. Material degradation within the damaged ply must be considered according to each failure mechanism for each ply. The degraded effective ply stiffness matrix can be presented as

$$[Q_{ij}^*] = \begin{bmatrix} Q_{11}^0 D_1 & Q_{12}^0 & 0 \\ Q_{12}^0 & Q_{22}^0 D_2 & 0 \\ 0 & 0 & Q_{66}^0 D_6 \end{bmatrix}, \quad (5)$$

where D_1, D_2 and D_6 are the material degradation factors that depend on each damage variable. The correlations between the material degradation factor D_i and damage variable FV_i are shown in Table 2. In this study, in order to take into account the effect of mixture damage mode on stiffness reduction in the model, a two-stage stiffness reduction is proposed to treat the degradation factor D_1 . Here, D_1 is divided into two values, D_1^{1st} and D_1^{2nd} , according to the damage mode. The latter will be used when FV_i satisfy a mixture damage mode condition, i.e. $FV_1 = FV_2 = 1$. The degraded effective ply material properties are presented in Appendix. The degradation factors (D_i) can be examined from a numerical parameter study (see Section 5.1).

Table 2.

Correlation of the material degradation factor D_i and damage variable FV_i

Failure state	Damage variable		Material properties			
	FV_1	FV_2	E_1	E_2	ν_{12}	G_{12}
No failure	0	0	E_1	E_2	ν_{12}	G_{12}
MTRX/comp. failure	1	0	E_1	$D_2 E_2$	$D_2^{-1} \nu_{12}$	$D_6 G_{12}$
FIB/comp-shear failure	0	1	$D_1^{1st} E_1$	$D_2 E_2$	$D_2^{-1} \nu_{12}$	$D_6 G_{12}$
MTRX/comp. and FIB/comp-shear failure	1	1	$D_1^{2nd} E_1$	$D_2 E_2$	$D_2^{-1} \nu_{12}$	$D_6 G_{12}$

4. FINITE ELEMENT ANALYSIS

4.1. FEA model

Consider the problem of the middle lap in a double shear-lap mechanically fastened joint (see Fig. 1). A laminated composite plate is loaded with an in-plane load P for the pinned-joint. A two-dimensional finite element model is constructed. Due to the symmetry of the analytical model, only one-half of the laminated plate is modeled and symmetry boundary conditions are imposed. The effect of the number of elements for different mesh design around the hole is also studied. The summary of finite element meshes and boundary conditions are shown in Fig. 3. A $[45/0/-45/90]_{2s}$ laminated plate is modeled in four-layers using 4-node plane stress element (CPS4R).

For the simplicity of the contact problem between the pin and the laminated plate, the pin circumference is modeled as a rigid surface, while the edge of the hole is modeled as a deformable surface. Note that the major objective of this work is to study damage progression analysis. Therefore, both friction and pin clearance will be negligible. The details of frictional contact analysis around the hole of pinned composite joints can be found in Ref. [14]. A tensile load is applied at the central node of the pin in the x -direction and the top edge of laminate is fixed in the x -direction. The material properties of the unidirectional CF/PIXA composites used in the analysis are shown in Table 3.

4.2. Algorithm using a program ABAQUS

The progressive failure analysis has been implemented through the user subroutine USDFLD of the commercial FEM code ABAQUS [15, 16]. This subroutine can be used to introduce solution-dependent material properties. The material properties depend on two field variables (FV_1, FV_2) that can be calculated from a set of failure criteria. Moreover, the values of the failure indices can be stored as solution-dependent state variables (note SDV in ABAQUS). The outline of the simulation process is as follows:

Step 1: User enters the analytical model data, such as the geometry, material properties and boundary conditions.

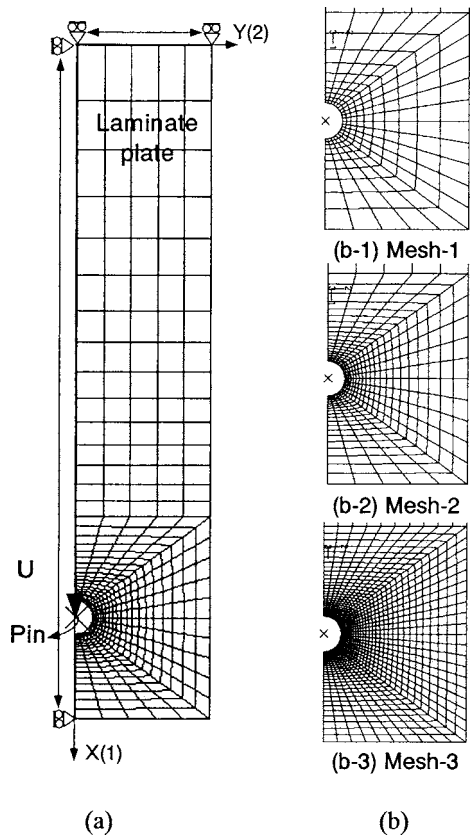


Figure 3. Finite element model, (a) a typical finite element mesh and boundary conditions, (b) various mesh design around hole.

Table 3.
Material properties of CF/PIXA lamina

Elastic properties of CF/PIXA	
Longitudinal modulus, E_1 (GPa)	152.4
Transverse modulus, E_2 (GPa)	8.06
Shear modulus, G_{12} (GPa)	4.69
Poisson's ratio, ν_{12}	0.34
Strength properties of CF/PIXA	
Longitudinal tensile strength, X_t (MPa)	2293
Longitudinal compression strength, X_c (MPa)	948.2
Transverse tensile strength, Y_c (MPa)	66.2
Transverse compression strength, Y_c (MPa)	210
In-plane shear strength, S_c (MPa)	155.3

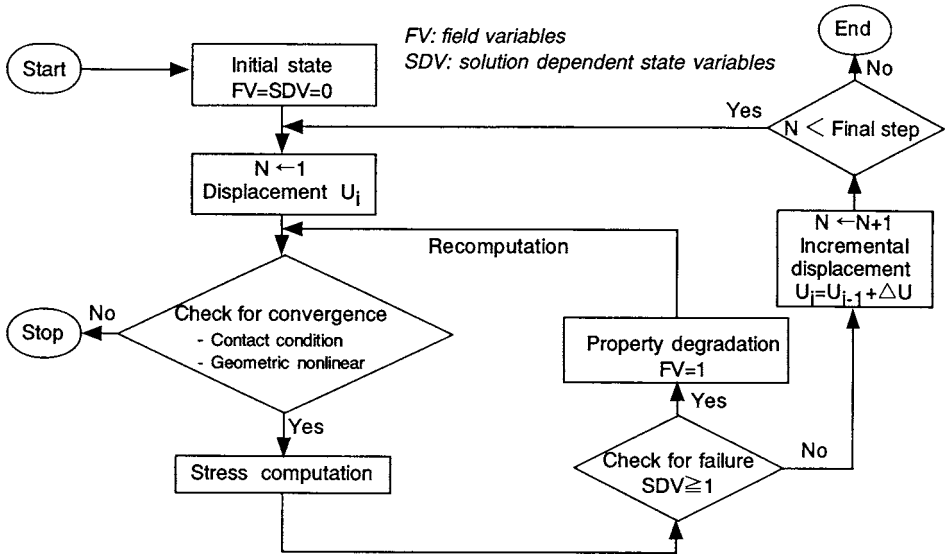


Figure 4. Flowchart of a two-dimensional progressive damage simulation.

- Step 2: Initial load by means of a compulsion displacement is applied at the central node of the pin. The convergence states for the contact condition and geometric nonlinearity are verified.
- Step 3: Based on equation (3), the stress is computed at the integration points of each element for the laminated plates.
- Step 4: Failure indices are computed using failure criteria tabulated in Table 1.
- Step 5: Once damage is predicted, effective material properties are updated according to each failure mode and state at the ply level, as shown in Table 2. The deformations and stresses are recalculated at the same loading level.
- Step 6: Step 3, 4 and 5 are repeated until new damage is not observed. The loading increment is reset back to Step 2, and the process from Step 2 to 5 is repeated until the last loading step.

This procedure is diagrammatically described by a flowchart shown in Fig. 4.

5. NUMERICAL RESULTS AND DISCUSSION

5.1. Determination of degradation factor D_i

The material degradation factors (D_i) are treated as the constants depending on the damaged state at the ply level, which is described in Subsection 3.3. They are assumed as constants in the same material system, and independent of the laminate lay-ups. It is also assumed that the different mesh design of the local elements will affect the computed result, because the global structural response is quite sensitive

to the cracked element. Therefore, we need to examine the following problems, in order to determine the material degradation factors D_i with a simpler and practical method:

- (1) The type and number of degradation factors D_i that should be determined are reduced maximally, and
- (2) The effect of the element size on analytical result is clarified.

In general, in-plane failure in the laminated plate can be globally classified into matrix cracking and fiber breakage. However, a damaged ply in laminate caused by compressive loading may have a different mechanism for transferring load than that caused by the tensile loading. Under the tensile loading the crack surfaces are traction free, but under compressive loading the crack surface can still carry the load (see Tan and Perez [11] where similar observations were reported). Therefore, the factor D_1 is more important than D_2 and D_6 under compressive loading, since the change of the stiffness along the fiber direction predominates in load carrying capability. Here, the material degradation factors D_2 and D_6 induced by matrix cracks were assumed to have a constant value, and these factors have been studied by Tan and Perez [11], for the problem of a laminate with a hole under compressive loading, which was approximately $D_2 = D_6 = 0.3$. This work will be to study mainly the material degradation factor D_1 .

For the determination of the stiffness degradation factor D_1 , it can be divided into two values, D_1^{1st} and D_1^{2nd} according to the damage state, which is described in Subsection 3.3. The determination procedure of D_1^{1st} and D_1^{2nd} can be discussed as follows:

- (a) The factor D_1^{1st} changes from 0.07 to 0.2, and the strength responses of the joint are computed using three kinds of element sizes. Then the optimum element mesh is decided and the estimation of load in initial damage is confirmed.
- (b) D_1^{2nd} changes as the multiples of D_1^{1st} , and this modifies D_1^{1st} value until the predicted results have improved more compared with the experimental data.

Note that no theoretical study has been conducted to evaluate the stiffness degradation factor D_1 under bearing loading, and so, it will be numerically determined.

A series of results is shown in Fig. 5. Figure 5a shows the effects of change of D_1^{1st} and element size on the P - δ curve. For $D_1^{2nd} = (D_1^{1st})^2$, D_1^{1st} changes from 0.07 to 0.2. Three kinds of element meshes, designated as Mesh-1, Mesh-2 and Mesh-3, are shown in Fig. 3b. The element meshes were created by a radial distribution from the center of the hole, and the differences of them were only on the change of the element sizes. Three types of element meshes were employed that have 250, 475 and 1300 elements, as well as 292, 532 and 1382 nodes, respectively.

In Fig. 5a, it was found that the response of strength is strongly affected by the change of D_1^{1st} value in the initial damage stage; but, the effect of the element sizes on the strength response was small. In the analysis, Mesh-2 was determined to be the optimum element mesh because of constraint in the calculation cost.

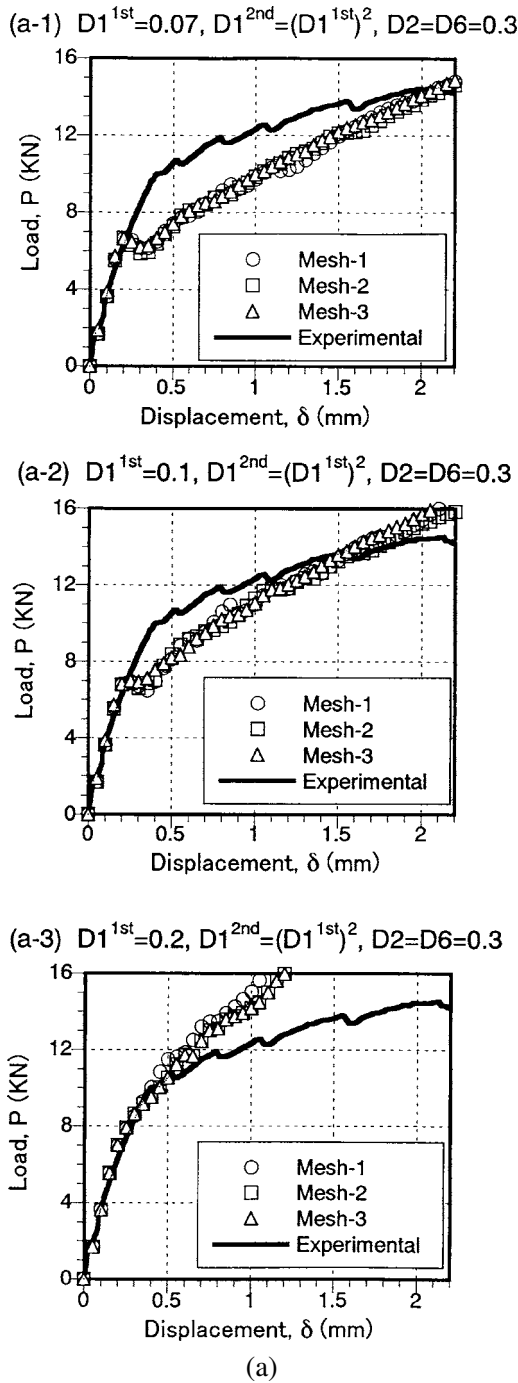


Figure 5. A series of discussion results for determining the stiffness degradation factor D_1^{1st} and D_1^{2nd} , (a) for determination of D_1^{1st} and discussion of the effect of element size, (b) determination of D_1^{2nd} using Mesh-2.

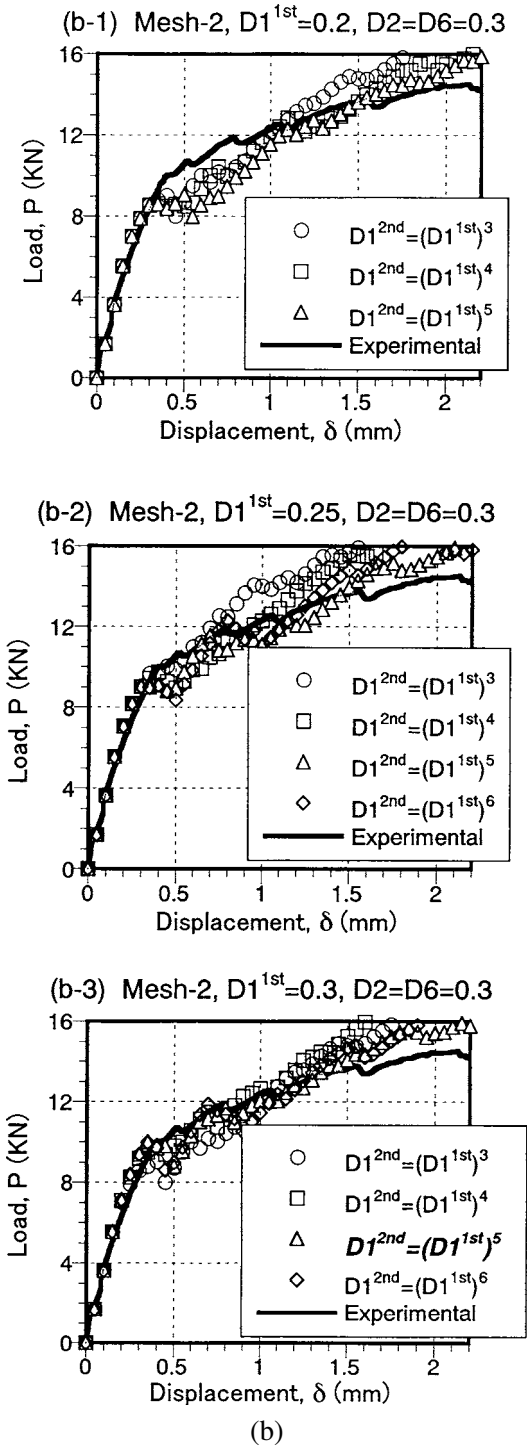


Figure 5. (Continued).

Figure 5b present a series of discussion results for D_1^{2nd} , which is changed as the multiples of D_1^{1st} (from 3rd to 6th power) using the finite element mesh Mesh-2. In Fig. 5b-1, because the strength response in the initial damage stage was lower than the experiment data for the case of $D_1^{1st} = 0.2$, it is necessary to modify D_1^{1st} . Figures 5b-2 and b-3 show the results that modified D_1^{1st} . The effect of the changes of D_1^{2nd} on the strength response during the damage progression stage was remarkable in all the cases presented here. Furthermore, modified D_1^{1st} is critical for the prediction of the initial damage response prediction. From above, it was found that the case of $D_1^{1st} = 0.3$ and $D_1^{2nd} = (D_1^{1st})^5$ as shown in Fig. 5b-3 agreed well with the existing experimental data.

5.2. Verifications and comparisons

In order to verify the effectiveness of the proposed analytical model, the reproducibility of the simulation results in CF/PIXA composite joints was compared with the experimental data in both the strength response and damage pattern.

Figure 6 presents the comparison of the calculated and experimentally measured load–displacement curves leading up to the ultimate failure. In the comparison, Mesh-2 is used with $D_1^{1st} = 0.3$, $D_1^{2nd} = (D_1^{1st})^5$ and $D_2 = D_6 = 0.3$. The experimental data for the elongations of the hole in the bolted joint specimen was measured from a non-contact electro-optical extensometer [17]. Overall, the predicted curves agreed with the experimental data very well, not only in the initial damage stage, but also the final structural failure of the CF/PIXA composite joints.

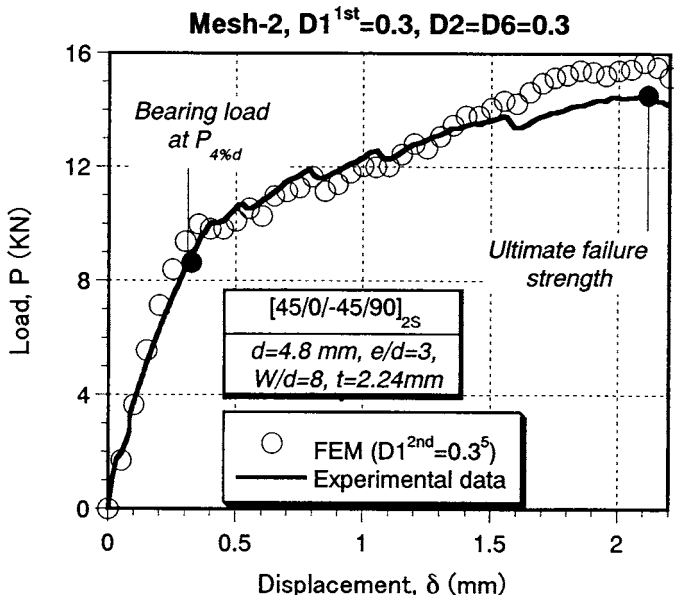


Figure 6. Comparison between experimental and numerical load–displacement curve for CF/PIXA specimens.

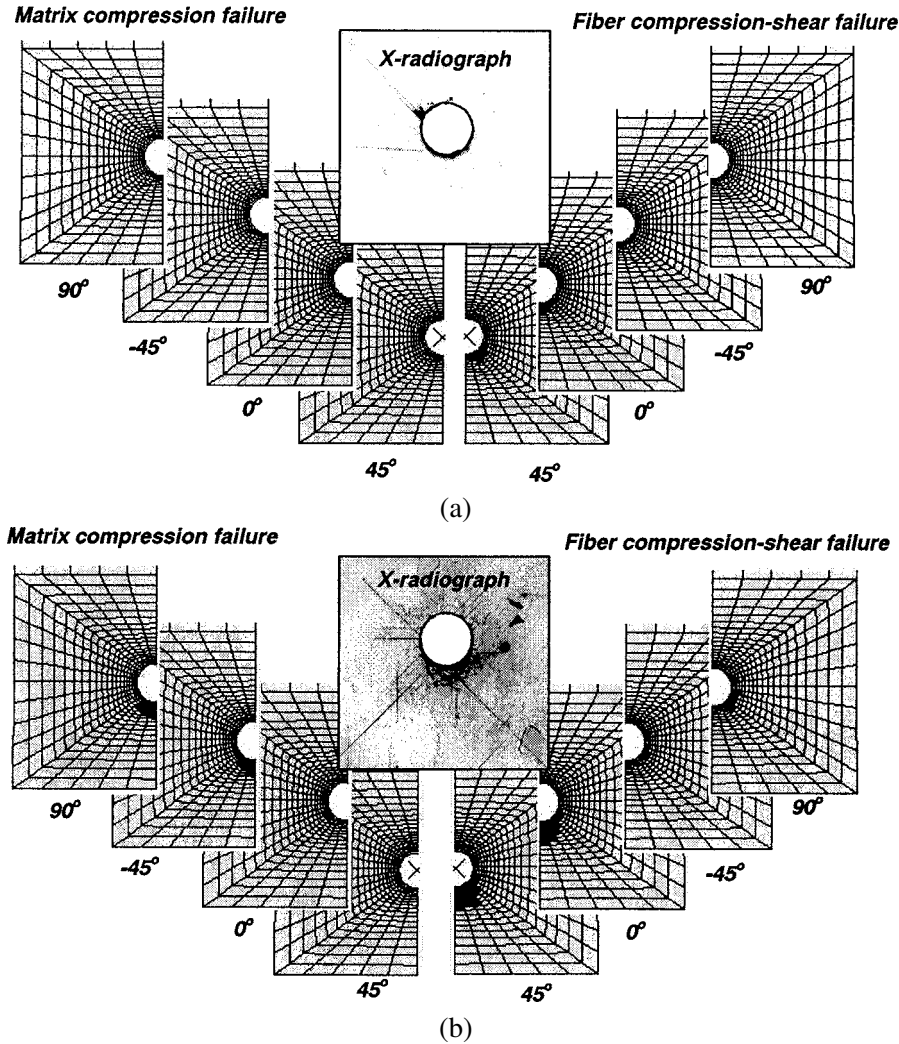


Figure 7. Comparison between experimental and numerical damage progression for different load stages and failure modes, loading at (a) $P = 8$ kN, (b) $P = 10$ kN, (c) $P = 12$ kN and (d) $P = 16$ kN.

Note that the significantly nonlinear behavior appearing in the load–displacement curve can be attributed to both the nonlinear shear deformation of materials and the degradation of mechanical properties resulting from the local damage in each ply.

For the CF/PIXA composite joints, the comparison of the predicted damage growth patterns as a function of the applied load with a set of X-ray radiographs tested specimens is shown in Fig. 7. The damage pattern was plotted by different damage modes at each ply, and the applied load was obtained as a reaction of central node of the pin. The predicted damage progression showed qualitatively the similar tendency and agreed with the experimental results. However, the bearing failure process is very complex as described in Section 2, and the internal damage

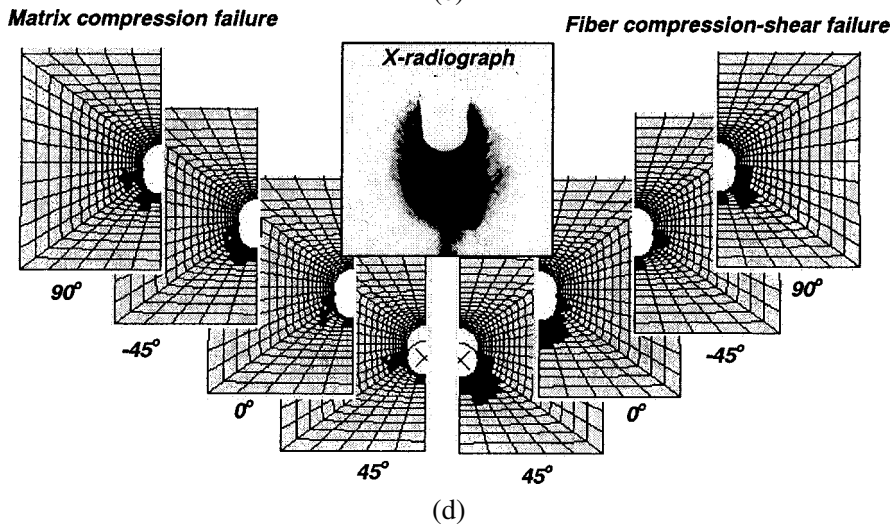
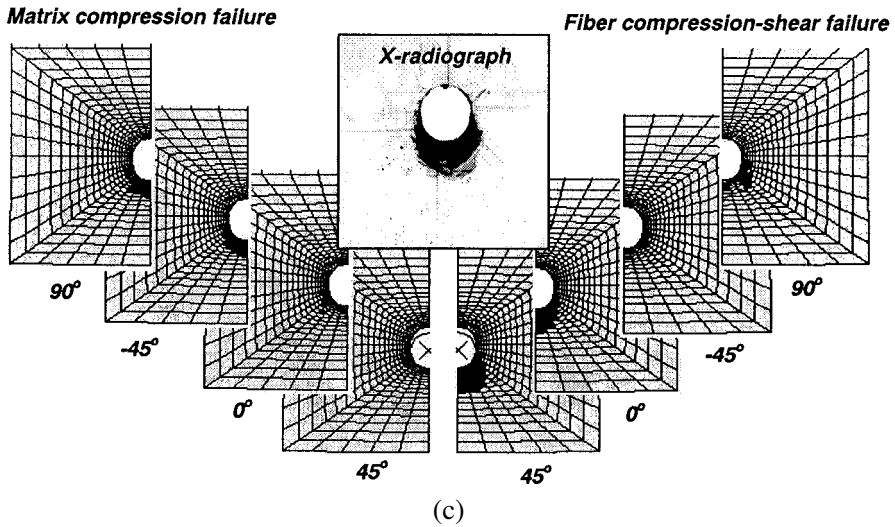


Figure 7. (Continued).

shown in X-ray radiograph will be a mode of multiple damages including the in-plane or out-of-plane failure mechanisms such as matrix cracking, fiber buckling, through-thickness shear cracks and delamination. For these reasons, the numerical simulations can evaluate only the in-plane ply failure, and not the out-of-plane ply failure.

6. CONCLUSIONS

An analytical tool was developed that can be employed to predict the in-plane response of laminated composite joints. The reproducibility of the numerical

simulations in CF/PIXA composite joints was compared with the experimental data from both the strength response and damage pattern. Based on this study, the following concluding remarks can be made:

- (1) It is effective to use two nonlinear algorithms in the model, containing the nonlinear shear deformation of materials without damage and the degradation of mechanical properties resulting from the local damage.
- (2) The effect of the stiffness degradation factors D_1^{1st} and D_1^{2nd} on the strength and response of the joints appear to be very significant.
- (3) A developed analytical tool that can provide the information of damage progression as a function of applied load is essential for the design of optimal composite joints.
- (4) Implementing a three-dimensional failure analysis to evaluate the through-the-thickness effect that includes the out-of-plane shear cracks, delamination and lateral constraint should be considered in our future work.

REFERENCES

1. J. L. Chaboche, Continuum damage mechanics: Part I — General concepts and Part II — Damage growth, crack initiation and crack growth, *J. Applied Mech.* **55**, 59–72 (1988).
2. F. K. Chang and K. Y. Chang, Post-failure analysis of bolted composite joints in tension or shear-out mode failure, *J. Compos. Mater.* **21**, 809–833 (1987).
3. L. B. Lessard and M. M. Shokrieh, Two-dimensional modeling of composite pinned-joint failure, *J. Compos. Mater.* **29**, 671–697 (1995).
4. C. L. Hung and F. K. Chang, Bearing failure of bolted composite joints. Part II: model and verification, *J. Compos. Mater.* **30**, 1359–1400 (1996).
5. S. J. Kim, J. S. Hwang and J. H. Kim, Progressive failure analysis of pin-loaded laminated composites using penalty finite element method, *AIAA J.* **36** (1), 75–80 (1998).
6. P. P. Camanho and F. L. Matthews, A progressive damage model for mechanically fastened joints in composite laminates, *J. Compos. Mater.* **33**, 2248–2280 (1999).
7. Y. Xiao and T. Ishikawa, Relationship between bearing strength and damage progress behavior of mechanically fastened joints in CFRP composites, *J. Japan Soc. Compos. Mater.* **28** (2), 56–65 (2002) (in Japanese).
8. T. Ishikawa, M. Matsushima and Y. Hayashi, Hardening non-linear behavior in longitudinal tension of unidirectional carbon composite, *J. Mater. Sci.* **20**, 4075–4083 (1985).
9. H. T. Hahn and S. W. Tsai, Nonlinear elastic behavior of unidirectional composite laminae, *J. Compos. Mater.* **7**, 102–118 (1973).
10. F. K. Chang and L. B. Lessard, Damage tolerance of laminated composites containing an open hole and subjected to compressive loadings: Part I — analysis, *J. Compos. Mater.* **25**, 2–43 (1991).
11. S. C. Tan and J. Perez, Progressive failure of laminated composites with a hole under compressive loading, *J. Reinf. Plast. Compos.* **12**, 1043–1057 (1993).
12. Z. Hashin, Failure criteria for unidirectional fiber composites, *J. Applied Mech.* **47**, 329–334 (1980).
13. S. E. Yamada and C. T. Sun, Analysis of laminate strength and its distribution, *J. Compos. Mater.* **12**, 275–284 (1978).
14. Y. Xiao, W. X. Wang, Y. Takao and T. Ishikawa, The effective friction coefficient of a laminate composite, and analysis of pin-loaded plates, *J. Compos. Mater.* **34**, 69–87 (2000).

15. ABAQUS/Standard version 5.8, *User's Manual*, HKS Inc., USA (1998).
16. ABAQUS/Standard version 5.8, *Example Problem Manual*, HKS Inc., USA, I: 3.2.25 (1998).
17. Y. Xiao and T. Ishikawa, Non-contact measurement for bearing strength of mechanically fastened joints in CFRP composites, *J. Japan Soc. Compos. Mater.* **26** (6), 213–218 (2000) (in Japanese).

APPENDIX

For the equation (3), the following relations exist between the engineering constants and the components of modulus of each undamaged ply:

$$\begin{aligned} Q_{11}^0 &= m E_1^0, & Q_{22}^0 &= m E_2^0, \\ v_{12}^0 &= \frac{Q_{12}^0}{Q_{22}^0}, & Q_{66}^0 &= G_{12}^0, \end{aligned} \quad (\text{A.1})$$

where

$$m = \left[1 - \frac{Q_{12}^0 Q_{21}^0}{Q_{11}^0 Q_{22}^0} \right]^{-1}.$$

Therefore, the effective engineering constants Q_{ij}^* of each damaged ply shown in equation (5) can be expressed as follows:

$$\begin{aligned} Q_{11}^* &= m E_1^0 D_1, & Q_{22}^* &= m E_2^0 D_2, \\ v_{12}^* &= \frac{Q_{12}^0}{Q_{22}^*} = v_{12}^0 D_2^{-1}, & Q_{66}^* &= G_{12}^0 D_6. \end{aligned} \quad (\text{A.2})$$

Note that it was assumed that m is independent of the damaged ply.